

Article

PbMoO₄ Synthesis from Ancient Lead and Its Single Crystal Growth for Neutrinoless Double Beta Decay Search

Arshad Khan ¹, Pabitra Aryal ¹, Hongjoo Kim ^{1,*}, Moo Hyun Lee ^{2,3}, Yeongduk Kim ^{2,3},

¹ Department of Physics, Kyungpook National University, Daegu 41566, Korea; kharshadmsc85@gmail.com (A.K.); shpbi@gmail.com (P.A.); hongjoo@knu.ac.kr (H.K.);

² Center for Underground Physics, Institute for Basic Science (IBS), Daejeon, 34126, Korea; mhlee@ibs.re.kr (M.L.); ydkim@ibs.re.kr (Y.K.);

³ IBS school, University of Science and Technology (UST), Daejeon 34113, Korea.

* Correspondence: hongjoo@knu.ac.kr

Abstract: A powder synthesis of PbMoO₄ from ancient lead (Pb) and deeply purified commercial MoO₃ powders was performed using a wet chemistry technique to achieve the low radioactivity scintillator for neutrinoless double beta decay search in ¹⁰⁰Mo. The synthesized powders were used to grow single crystals of PbMoO₄ by a Czochralski technique in Ar environment. The luminescence and scintillation properties were measured with excitations using UV, X- and γ -rays in temperature range of 10–300 K. Annealing of the grown PMO crystal in air atmosphere enhanced the scintillation light yield by ~3 orders of magnitude compared to that measured before annealing. The scintillation light yield of grown PMO crystal at 10 K is found to be 127% to that of a reference PMO crystal under 662 keV γ -rays excitation from a ¹³⁷Cs source. The background measurement of the grown crystal performed at 50 K shows negligible activity from ²¹⁰Pb compared to that of reference PMO crystal. These preliminary performances show that the PMO crystal grown from ancient Pb and deeply purified MoO₃ powders has the great potential to be used as cryogenic scintillator for the neutrinoless double beta decay search in ¹⁰⁰Mo.

Keywords: ancient Pb; synthesis; single crystal growth; scintillation; thermally stimulated luminescence

1. Introduction

PbMoO₄ (PMO) is one of the extensively studied material because of its wider applications in acousto-optics [1], optoelectronics [2], photocatalysis [3], and high voltage measuring devices. Single crystal growth of PMO by Czochralski technique were reported elsewhere in references [4–9]. The difficulties arose during crystal growth from bubble formation [10], compositional changes due to evaporation of the volatile MoO₃ powders [11], cracking of the crystal during and after growth and coloration which deteriorates the optical quality of the crystal were extensively studied and reported [12,13]. Moreover, the crystal growth with improved optical quality was reported by the low thermal gradient Czochralski technique [7].

PMO belongs to scheelite structure family of crystal with space group I4₁/a [14]. The single crystals belonging to this family were widely studied due to its common luminescence features, for the applications in high energy physics, dark matter and double beta decay searches [15–20]. The interest in the application of molybdates single crystalline scintillators arose from the introduction of cryogenic phonon scintillation detectors (CPSD) in the search for neutrinoless double beta ($0\nu\beta\beta$) decay. Advantages of CPSD over other detectors are good particle discrimination capability and high energy resolution [21,22]. This detection technique is under usage by AMoRE [22] and CUPID-Mo

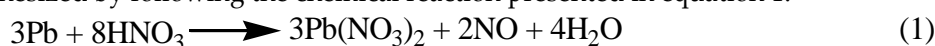
[23] experiments for the $0\nu\beta\beta$ decay in ^{100}Mo . These experiments are using $^{40}\text{Ca}^{100}\text{MoO}_4$ and $\text{Li}_2^{100}\text{MoO}_4$ cryogenic scintillators, however, because of the purification limitation of Ca and low light output of LMO the search for novel scintillators with improved scintillation performance, low internal background and capability that can be grown easily in large volume are desired [24]. The scintillation performance tests of PMO crystal were carried out to check the feasibility for dark matter and $0\nu\beta\beta$ decay searches [17,19,20]. However, the intrinsic background imposed by ^{210}Pb in the PMO crystal grown from commercial precursors limits its applications in rare event search experiments [20]. This intrinsic background can be reduced by utilizing the ancient Pb for the powder synthesis and hence PMO crystal growth. The low radioactivity archeological Pb was used to synthesize PbO powders which mixed with MoO_3 powders for the growth of PMO crystal by low thermal gradient Czochralski technique [7]. Scintillation bolometric performance of this archeological PMO shows excellent performance, however, suffered from huge internal radioactivity due to the dropping of a ceramic piece during crystal growth [18]. Therefore, careful handling during powder synthesis and crystal growth is required to avoid this issue.

This study focuses on the powder synthesis of PMO directly from the ancient Pb, commercial and deeply purified MoO_3 powders by a wet chemistry technique for the 1st time. The synthesized powders were used to grow single crystals of PMO by a Czochralski technique in Ar atmosphere. The phase of the grown PMO crystals were confirmed by powders using X-ray diffraction analysis. The comparative analysis of the grown crystals was evaluated by 4.42 eV excitation. The scintillation performance of the PMO crystal grown from powders synthesized from ancient Pb and deeply purified MoO_3 powders was studied under γ -rays excitation in the temperature range of 300-10 K and compared with a reference PMO crystal. Moreover, the effect of annealing in air atmosphere on the scintillation properties of the grown crystal was studied under γ -rays excitation. Thermally stimulated luminescence (TSL) measured after X-ray irradiation at 10 K shows multiple traps which causes the quenching of light yield at low temperature due to the self-trapping of electrons at $(\text{MoO}_4)^{2-}$ complexes.

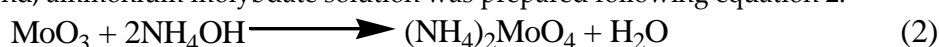
2. Materials and Methods

2.1 Powders synthesis

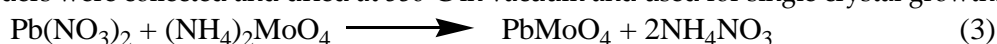
Low radioactivity ancient Pb (T2FA, Lemer Pax, France) has been being used for the detector shielding in AMORE [22] and other rare event search experiments [25]. Moreover, this Pb has been utilized for the fabrication of low radioactivity Pb-Sn alloy which serves as soldering material in the cryogenic detector construction in AMORE experiment. The low radioactivity of the ancient Pb has been being investigated recently by the cryogenic detection technique which is the most sensitive for this measurement and reported the ^{210}Pb concentration to be lower than 715 $\mu\text{Bq/kg}$ [25]. Such low activity of the ancient Pb is quite encouraging for its utilization in PMO synthesis. For this purpose, the ancient Pb block was cut in small pieces, cleaned by HNO_3 and dried. The dried Pb pieces were used to synthesize two different batches of PMO powders by wet chemistry technique. The 1st batch of PMO powders was synthesized from ancient Pb and commercial MoO_3 (Alfa Aesar) while the 2nd batch from ancient Pb and deeply purified MoO_3 powders. The purification procedure and its intrinsic radioactivity results were published elsewhere in reference [26]. First, $\text{Pb}(\text{NO}_3)_2$ was synthesized by following the chemical reaction presented in equation 1:



Second, ammonium molybdate solution was prepared following equation 2.



Extra amount of MoO_3 (5% by weight) than theoretical requirement according to equation 3 was used to synthesis PMO. The solution of $\text{Pb}(\text{NO}_3)_2$ was added dropwise to the solution of $(\text{NH}_4)_2\text{MoO}_4$ under continuous stirring with magnetic stirrer. Immediately white powders were precipitated. The powders were collected and dried at 550°C in vacuum and used for single crystal growth.



Extra amount of molybdenum remains in NH_4NO_3 solution which was recovered from the waste solution by adjusting pH of the solution as 2 using HNO_3 acid. The detail description of the PMO powder synthesis procedure is illustrated in Figure 1.

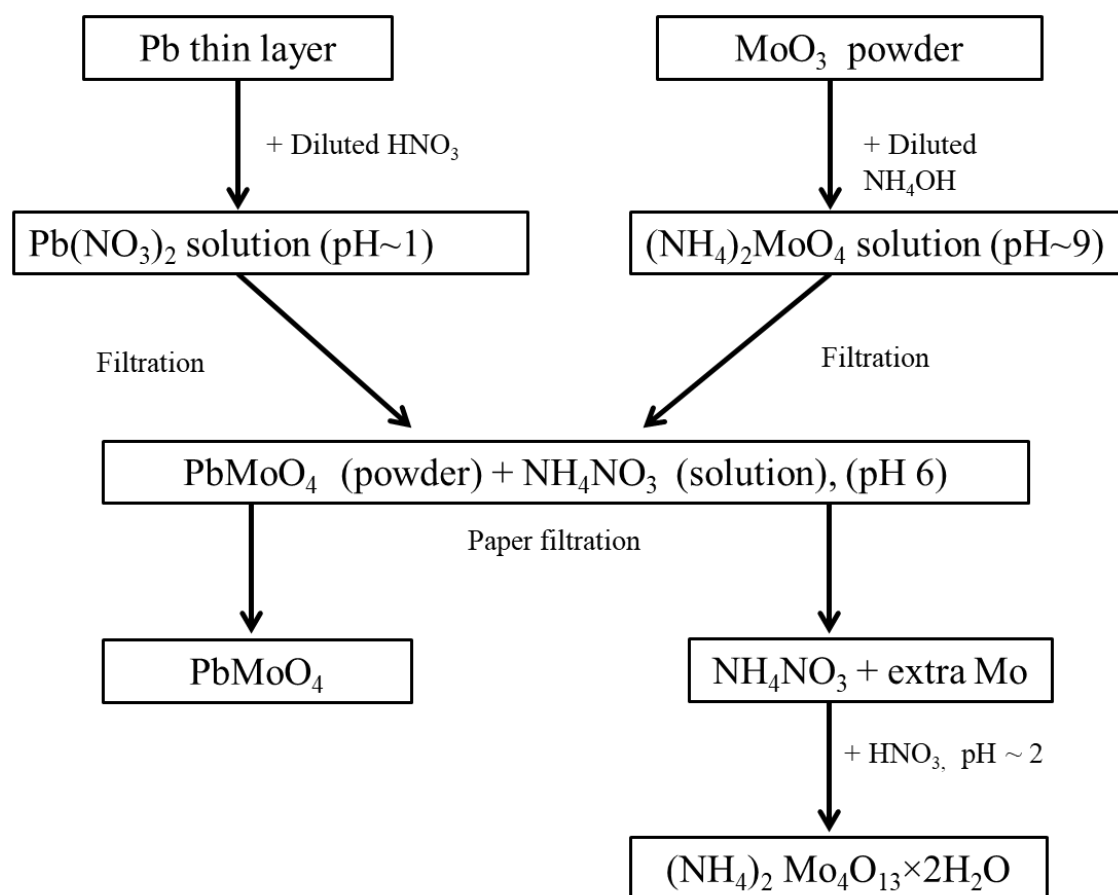


Figure 1. Flow chart of the necessary steps employed for the synthesis of PMO powder.

2.2 Crystal growth

A conventional Czochralski method was used for the single crystal growth of PMO crystals from the synthesized powders. The 1st batch of PMO powders were loaded to a platinum crucible having diameter and height of 3 cm respectively. The crucible was transferred to Czochralski chamber and melted the powders with radio frequency heating in Ar atmosphere. The temperature was controlled by a thermocouple connected to the bottom of the crucible. After complete melting, the PMO seed was slowly lowered to the melt and grow the crystal with growth and rotation rate of 1 mm/h and 10 rpm respectively. In this way PMO crystals from 1st and 2nd batches of powders were grown with diameter of ~15 mm and length of 40 mm as shown in Figure 2. The PMO crystal

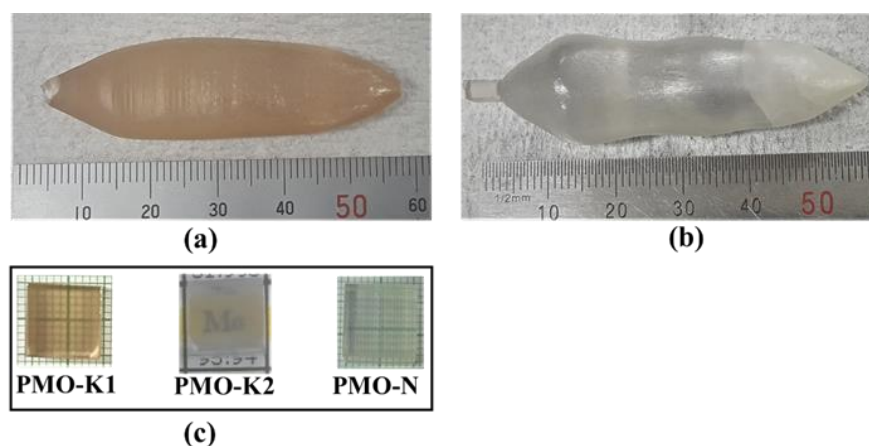


Figure 2. Photographs of PMO crystals grown from (a) 1st batch, (b) 2nd batch of synthesized powders and (c) 10 mm × 10 mm × 10 mm polished samples from crystals grown from 1st, 2nd batch powders and that received from NIIC.

grown from 1st batch of powders had dark yellow color (Figure 2a) due to the low purity of MoO₃ powders. This coloration effect in PMO crystal was previously studied with different purity grade starting materials and was attributed to extrinsic impurities present in the starting materials [13]. Although we did not measure the extrinsic impurities concentrations in the grown crystal, however, in analogy, we can attribute this coloration due to the same origin. Our assumption is further supported from the colorless PMO crystal (Figure 2b) grown from the 2nd batch of powders which was prepared from ancient Pb and deeply purified MoO₃ powders. Samples of 10 mm × 10 mm × 10 mm were cut from the grown crystals using diamond coated stainless steel wire saw and optically polished for various characterizations. The grown crystals were compared with a 10 mm × 10 mm × 10 mm PMO sample from Nikolaev Institute of Inorganic Chemistry (NIIC) which was grown by low thermal gradient Czochralski technique from commercially available modern PbO and sublimed MoO₃ powders. The sample grown at our laboratory from 1st batch, 2nd batch powders and from NIIC were labeled as PMO-K1, PMO-K2 and PMO-N respectively as shown in Figure 2(c).

2.3 Characterizations

The grown PMO crystals were characterized by X-ray powder diffraction (XRD) analysis for confirmation of phase using an XPERT-MED diffractometer. X-rays of wavelength 0.154 nm was generated from a Cu target with power of 40 kV and current of 30 mA. The XRD data were collected in the 2θ range from 10° to 70° with step size of 0.025° and scanning rate of 3 s/step. The recorded XRD data of the PMO crystals were refined using Material Analysis Using Diffraction (MAUD) software by Rietveld refinement method [27]. Luminescence of the grown crystals were measured in temperature range of 300-10 K using excitation of 4.42 eV from a light emitting diode (LED) source. The crystals samples were wrapped from three sides with several layers of 1 μm thick Teflon tape to improve light collection while the other three faces were kept bare for thermal coupling to the Cu sample holding plate, incident light from excitation source, and emission light collection respectively. Emitted lights from the crystal were collected through a quartz light guide by a calibrated QE65000 ocean optics fiber spectrometer. A schematic representation of the low temperature experimental setup used for luminescence measurement of PMO crystal is shown in Figure 3(a). The scintillation light yields of the grown and reference crystals were measured in

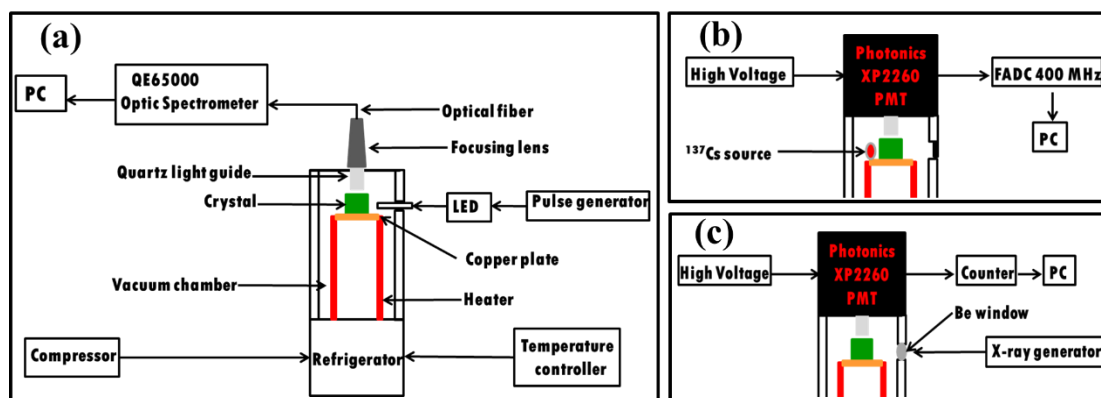


Figure 3. Schematic representations of low temperature experimental setups used for (a) luminescence, (b) scintillation, and (c) thermoluminescence measurements of PMO crystals.

temperature range of 300–10 K under 662 keV γ -ray excitations from a ^{137}Cs source. Four faces of the crystal sample except bottom for thermal coupling and top for light collection were wrapped with several layers of Teflon tape and placed in the cryostat. The ^{137}Cs source was also placed inside the cryostat at ~ 1 cm from the sample. A schematic representation of the low temperature scintillation measurement setup is presented in Figure 3(b). Lights from the crystal were fed to photocathode of XP2260 PMT through a quartz light guide. Signals from PMT were digitized with 400 MS/s FADC with a time window of 64 μs . An offline analysis of the recorded data was performed for scintillation light yield with a customized C++ code compiled and run in ROOT [28]. For TSL measurement the crystal sample was cooled down to 10 K and irradiated by X-rays through Be window, generated from a Cu anode. After irradiation the sample was heated at a rate of 0.1 K/s and TSL intensity through the XP2260 PMT was recorded by a homemade counter in temperature range of 10–300 K. The TSL measurement setup is shown schematically in Figure 3(c).

3. Results

The XRD results of the grown crystals measured at room temperature are shown in Figure 4(a–b) fitted with Rietveld refinement method. The Rietveld refinement shows good agreement between experimental data and theoretical results (Figure 4, a–b). The residue in Figure represents the difference between the experimental XRD profile and calculated data which is very close to zero in intensity scale. The wR_p values are less than 9% for both PMO crystals and are in the acceptable ($wR_p < 10\%$) range for a medium complex phase such as tetragonal [14]. Moreover, the Goodness of Fit (GOF) of 1.09 and 1.15 was obtained for PMO-K1 and PMO-K2 respectively showing good quality of the refinement. PMO crystallizes in scheelite type tetragonal structure with space group $I4_1/a$ with obtained lattice parameters of $a = 5.439 \text{ \AA}$, $c = 12.112 \text{ \AA}$ for PMO-K1 and $a = 5.437 \text{ \AA}$, $c = 12.114 \text{ \AA}$ for PMO-K2 which are in good agreement with that reported elsewhere in reference [14]. The detailed description about the structural refinement of PMO crystals grown with various methods can be found elsewhere in reference [14].

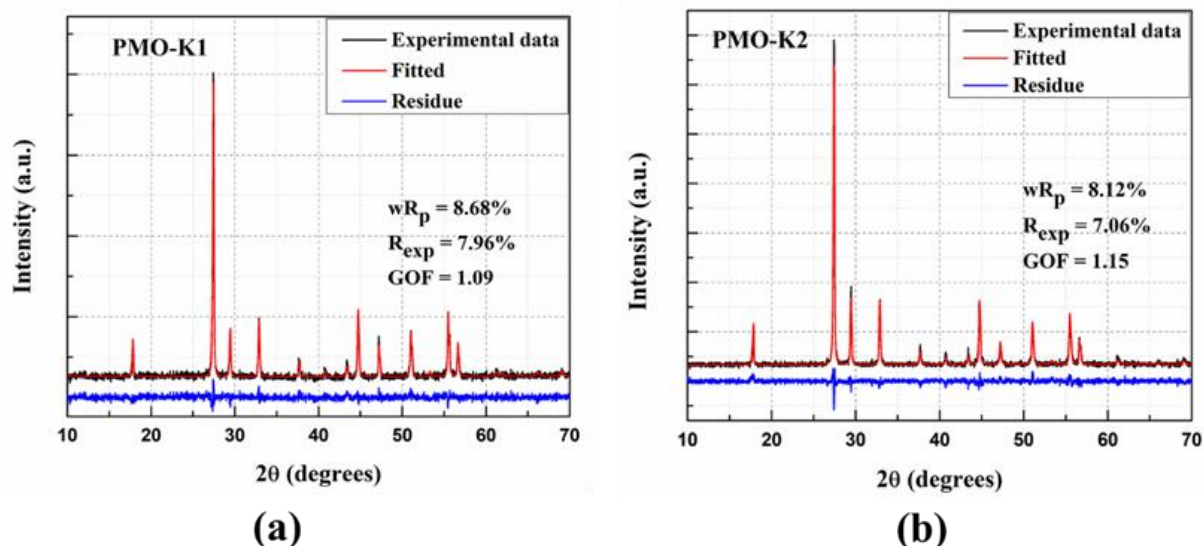


Figure 4. XRD patterns of (a) PMO-K1 and (b) PMO-K2 crystals.

Emission spectra of the grown PMO crystals at various temperatures are shown in Figure 5(a-b). Under excitation with 4.42 eV lights, these crystals showed weak luminescences at 200 K. Decreasing temperature of the crystal enhanced the luminescence having the highest intensity at 10 K (Figure 5,a-b). The emission spectra observed in this study have similar band as reported earlier in literatures with different excitation energies [19,29,30]. The emission spectra are composed of overlapping emission bands as shown in Figure 5(c). The deconvolution of the 420-900 nm band in the emission spectrum of PMO-K2 at 10 K shows two emission bands having maximum peaks at 515 nm and 575 nm respectively. These emission bands originate from degenerated triplet states $^3T_{1,2-1}A_1$ transitions of MoO_4^{2-} oxyanionic complexes. A short wavelength band at about 402 nm arose from the $^1T_{1,2-1}A_1$ singlet transition of MoO_4^{2-} complex [30]. Temperature dependence of the integrated luminescence intensities of PMO-K1, PMO-K2, and PMO-N measured under the same experimental conditions are shown in Figure 5(d). Luminescence intensities of all these crystals decreased upon increasing temperature above 75 K. Moreover, luminescence light yields at 10 K for PMO-K1 and PMO-K2 were measured to be 70% and 100% respectively to that of PMO-N. The decrease in luminescence intensity with increase in crystal temperature are assigned to the effect of thermal quenching due to the dominant non-radiative recombination process at high temperatures. Significance of non-radiative recombination processes reduces at low temperature and results in enhancement of light yield [16,31].

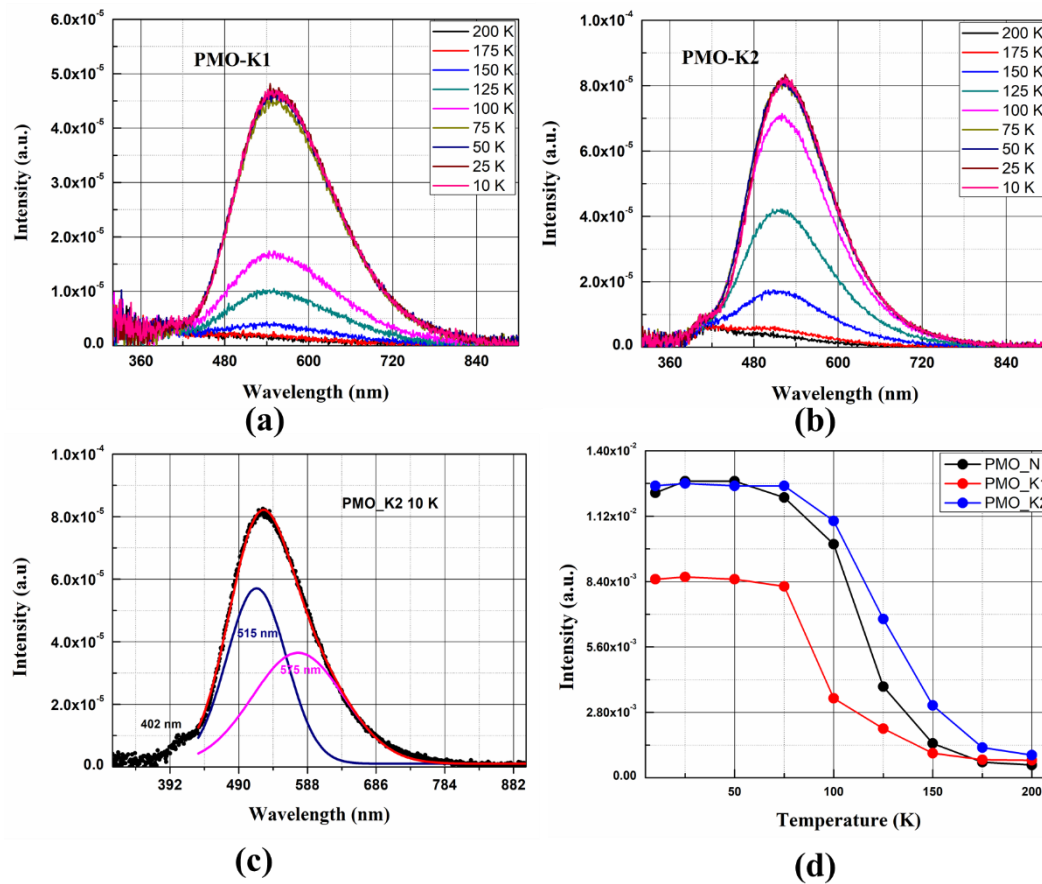


Figure 5. (a–b) Emission spectra of PMO-K1 and PMO-K2 respectively at different temperatures, (c) emission spectrum of PMO-K2 at 10 K deconvoluted by two Gaussian distribution functions and (d) temperature dependences of integrated luminescence intensities of PMO-K1 (red circles), PMO-K2 (blue circles) and PMO-N (black circles). All the measurements were performed under 4.42 eV excitation from an LED source.

Temperature dependence of scintillation light yield under excitation with 662 keV γ from a ^{137}Cs source is shown in Figure 6(a). The photopeak in pulse height spectrum was fitted with Gaussian function at each temperature and the mean channel number is plotted as a function of temperature.

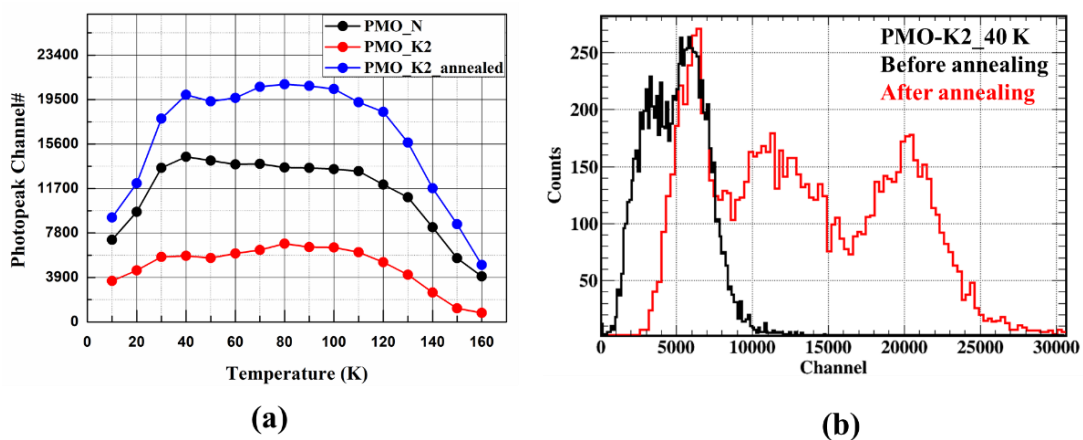


Figure 6. (a) Temperature dependence of scintillation light yields of PMO-K2 before (red circles) and after annealing (blue circles) in air atmosphere and PMO-N (black circles), (b) pulse height spectra of PMO-K2 before and after annealing measured at 40 K. All these measurements were performed under 662 keV γ -ray excitation from a ^{137}Cs source.

Light outputs were compared with PMO-N at all temperatures (Figure 6a). Temperature dependence of the light yield has a similar tendency for both crystals, i.e. enhanced upto 40 K and then quenched upon further cooling the crystals down to 10 K. Light yield of PMO-K2 at 10 K was calculated to be 50% of PMO-N before annealing. Growths of PMO crystals in Ar atmosphere create oxygen deficiencies. These oxygen deficiencies are acting as electron trapping centers and reduced the light yield when PMO crystal was excited with high energy photons. Therefore, annealing PMO-K2 crystal at 900 °C for 24 hours in air atmosphere reduced the concentration of oxygen deficiencies resulting in enhancement of light output to 127% of PMO-N at 10 K. As presented in Figure 6(b), light output shows an enhancement of ~3 orders of magnitude at 40 K after annealing. The decrease in scintillation light yield below 40 K can be understood from TSL glow curve. As can be seen from the TSL glow curve in Figure 7 measured after X-ray irradiation at 10 K, multiple traps at 39 K, 73 K and 106 K were observed like that reported earlier for PMO crystal [32]. Origin of these trap centers was investigated extensively by Electron

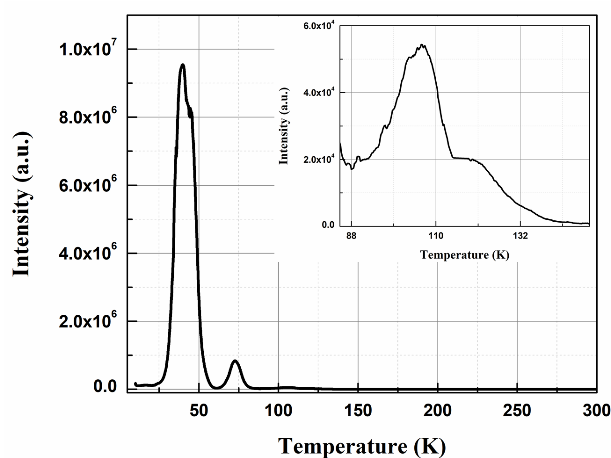


Figure 7. TSL glow curve of PMO-K2 measured after X-ray irradiation at 10 K and measured at heating rate of 0.1 K/s. The inset shows an enlarged view of 80-150 K region.

Paramagnetic Resonance (EPR) technique and high energy photon irradiation and reported in references [32–34]. The high intensity peak at ~40 K below which the light yield reduced significantly was assigned to trapping of electrons at $(\text{MoO}_4)^{2-}$ oxyanionic complexes [32]. Energy transfer to luminescence center influenced strongly by charge carriers trapping at trap centers. From temperature dependence of integrated luminescence intensity under 4.42 eV excitation (direct creation of excitons) no quenching at low temperatures were observed. However, light outputs under high energy 662 keV γ -ray excitations showed a steep drop below 40 K due to presence of trap centers at low temperatures. These trap centers are in competition with radiative recombination of charge carriers and responsible for quenching of light yield below 40 K [32].

To confirm low activity of grown PMO crystal from ^{210}Pb , the internal background measurement was carried out at 50 K under the low temperature experimental setup and compared with PMO-N. As shown in Figure 8(a), a large internal background peak of 5.3 MeV α was detected from ^{210}Po for PMO-N which contains non-ancient Pb. However, a signature of such background peak was not observed from PMO-K2 (Figure 8b) confirming low radioactivity of the crystal for ^{210}Pb as expected. The detail investigation of internal activity measurement of PMO grown from ancient Pb will be carried out at mK in the CPSD setup and will be reported elsewhere.

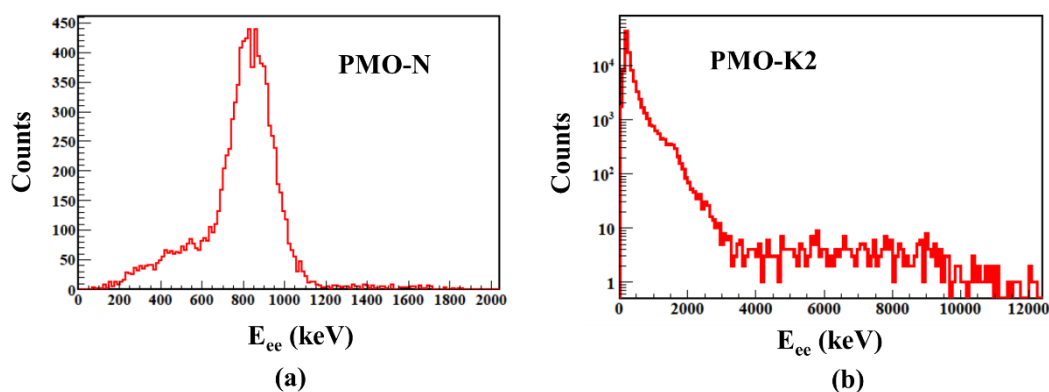


Figure 8. Total background spectra of (a) PMO-N and (b) PMO-K2 measured at 50 K.

5. Conclusions

A synthesis method for PMO powders from ancient Pb and deeply purified MoO₃ powders was successfully developed. A single crystal growth from the synthesized powders by a Czochralski technique resulted crack free PMO crystals. The grown crystals showed high phase purity as confirmed from XRD measurement. The dark yellow and white colors of PMO crystals grown from low grade and high purity powders respectively confirmed origin of colors due to impurities. Low temperature luminescence measurement reveals the identical emission bands as reported previously due to singlet T_{1,2} and triplet T_{1,2} states to ground state ¹A₁ transition of the (MoO₄)²⁻ complex. Low temperature scintillation light yield of PMO-K2 under 662 keV γ -ray excitation shows higher light yield than the reference PMO crystal after annealing in air atmosphere. Moreover, the quenching of scintillation light yield below 40 K was confirmed from TSL measurement due to presence of high intensity glow peak at low temperature and attributed to the trapping of charge carriers at these trap centers. An internal background measurement of PMO-K2 at 50 K shows low activity in ²¹⁰Pb. These investigations reveal great potential of PMO to be used for 0 $\nu\beta\beta$ decay search in ¹⁰⁰Mo. Further study on the PMO crystal as a bolometer at mK temperature is underway to fully investigate its feasibility for the 0 $\nu\beta\beta$ decay search.

Author Contributions: Conceptualization, A.K., P.A., H.K.; methodology, A.K., P.A.; validation, A.K., H.K.; formal analysis, A.K.; investigation, A.K., H.K.; resources, H.K.; data curation, A.K.; writing—original draft preparation, A.K.; M.L.; writing—review and editing, H.K., P.A., M.L.; visualization, A.K., H.K.; supervision, H.K.; project administration, H.K.; funding acquisition, H.K., Y.K., All authors have read and agreed to the published version of the manuscript.

Funding: These investigations have been funded by the Ministry of Science and Technology, Korea (MEST) (No. 2018R1A2A1A05022079) and IBS-R016-D1-2018-a01.

Conflicts of Interest: The authors declare no conflict of interest.

References

1. Chesler, R.B.; Pinnow, D.A.; Benson, W.W. Suitability of PbMoO₄ for Nd: YAIG Intracavity Acoustooptic Modulation. *1971*, *10*, 2562.
2. Damen, E.P.N.; Arts, A.F.M.; De Wijn, H.W. High-frequency monochromatic acoustic waves generated by laser-induced thermomodulation. *Phys. Rev. Lett.* **1995**, *74*, 4249–4252.
3. Hernández-Uresti, D.B.; Martínez-de la Cruz, A.; Torres-Martínez, L.M. Photocatalytic properties of PbMoO₄ synthesized by co-precipitation method: organic dyes degradation under UV irradiation. *Res. Chem. Intermed.* **2012**, *38*, 817–828.

4. Takano, S.; Esashi, S.; Mori, K.; Namikata, T. Growth of high-quality single crystals of lead molybdate. *J. Cryst. Growth* **1974**, *24–25*, 437–440.
5. Sabharwal, S.C.; Sangeeta; Desai, D.G. Investigations of single crystal growth of PbMoO₄. *Cryst. Growth Des.* **2006**, *6*, 58–62.
6. Senguttuvan, N.; Moorthy Babu, S.; Dhanasekaran, R. Some aspects on the growth of lead molybdate single crystals and their characterization. *Mater. Chem. Phys.* **1997**, *49*, 120–123.
7. Shlegel, V.N.; Borovlev, Y.A.; Grigoriev, D.N.; Grigorieva, V.D.; Danevich, F.A.; Ivannikova, N. V.; Postupaeva, A.G.; Vasiliev, Y. V. Recent progress in oxide scintillation crystals development by low-thermal gradient Czochralski technique for particle physics experiments. *J. Instrum.* **2017**, *12*.
8. Chen, H.; Ge, C.; Li, R.; Wang, J. Bridgman growth of lead molybdate crystals. *J. Mater. Sci.* **2006**, *41*, 5383–5385.
9. Senguttuvan, N.; Moorthy Babu, S.; Subramanian, C. Synthesis, crystal growth and mechanical properties of lead molybdate. *Mater. Sci. Eng. B* **1997**, *47*, 269–273.
10. Lim, L.C.; Tan, L.K.; Zeng, H.C. Bubble formation in Czochralski-grown lead molybdate crystals. *J. Cryst. Growth* **1996**, *167*, 686–692.
11. Sangeeta; Desai, D.G.; Singh, A.K.; Tyagi, M.; Sabharwal, S.C. Non-stoichiometry-induced cracking in PbMoO₄ crystals. *J. Cryst. Growth* **2006**, *296*, 81–85.
12. Zeng, H.C. Correlation of PbMoO₄ crystal imperfections to Czochralski growth process. *J. Cryst. Growth* **1997**, *171*, 136–145.
13. Tyagi, M.; Singh, S.G.; Singh, A.K.; Gadkari, S.C. Understanding colorations in PbMoO₄ crystals through stoichiometric variations and annealing studies. *Phys. Status Solidi Appl. Mater. Sci.* **2010**, *207*, 1802–1806.
14. Bomio, M.R.D.; Cavalcante, L.S.; Almeida, M.A.P.; Tranquilin, R.L.; Batista, N.C.; Pizani, P.S.; Siu Li, M.; Andres, J.; Longo, E. Structural refinement, growth mechanism, infrared/Raman spectroscopies and photoluminescence properties of PbMoO₄ crystals. *Polyhedron* **2013**, *50*, 532–545.
15. Mikhailik, V.B.; Kraus, H. Performance of scintillation materials at cryogenic temperatures. *Phys. Status Solidi Basic Res.* **2010**, *247*, 1583–1599.
16. Babin, V.; Bohacek, P.; Bender, E.; Krasnikov, A.; Mihokova, E.; Nikl, M.; Senguttuvan, N.; Stolovits, A.; Usuki, Y.; Zazubovich, S. Decay kinetics of the green emission in tungstates and molybdates. *Radiat. Meas.* **2004**, *38*, 533–537.
17. Nagornaya, L.L.; Danevich, F.A.; Dubovik, A.M.; Grinyov, B. V.; Henry, S.; Kapustyanyk, V.; Kraus, H.; Poda, D. V.; Kudovbenko, V.M.; Mikhailik, V.B.; et al. Tungstate and molybdate scintillators to search for dark matter and double beta decay. *IEEE Trans. Nucl. Sci.* **2009**, *56*, 2513–2518.
18. Nagorny, S.; Pattavina, L.; Kosmyrna, M.B.; Nazarenko, B.P.; Nisi, S.; Pagnanini, L.; Pirro, S.; Schaffner,

- K.; Shekhovtsov, A.N. $^{arch}\text{PbMoO}_4$ scintillating bolometer as detector to searches for the neutrinoless double beta decay of ^{100}Mo . *J. Phys. Conf. Ser.* **2017**, *841*, 012025.
19. Khan, A.; Daniel, D.J.; Kim, H.; Pandey, I.R.; Shlegel, V.; Lee, M.H.; Kim, Y. Luminescence and scintillation characterization of PbMoO_4 crystal for neutrinoless double beta decay search. *Radiat. Meas.* **2019**, *123*, 34–38.
 20. Danevich, F.A.; Grinyov, B. V.; Henry, S.; Kosmyna, M.B.; Kraus, H.; Krutyak, N.; Kudovbenko, V.M.; Mikhailik, V.B.; Nagornaya, L.L.; Nazarenko, B.P.; et al. Feasibility study of PbWO_4 and PbMoO_4 crystal scintillators for cryogenic rare events experiments. *Nucl. Instruments Methods Phys. Res. Sect. A Accel. Spectrometers, Detect. Assoc. Equip.* **2010**, *622*, 608–613.
 21. Kim, G.B.; Choi, S.; Danevich, F.A.; Fleischmann, A.; Kang, C.S.; Kim, H.J.; Kim, S.R.; Kim, Y.D.; Kim, Y.H.; Kornoukhov, V.A.; et al. A CaMoO_4 crystal low temperature detector for the AMoRE neutrinoless double beta decay search. *Adv. High Energy Phys.* **2015**, *2015*, 1–15.
 22. Jo, H.S.; Choi, S.; Danevich, F.A.; Fleischmann, A.; Jeon, J.A.; Kang, C.S.; Kang, W.G.; Kim, G.B.; Kim, H.J.; Kim, H.L.; et al. Status of the AMoRE Experiment Searching for Neutrinoless Double Beta Decay Using Low-Temperature Detectors. *J. Low Temp. Phys.* **2018**, 1–8.
 23. Armengaud, E.; Augier, C.; Barabash, A.S.; Bellini, F.; Benato, G.; Benoît, A.; Beretta, M.; Bergé, L.; Billard, J.; Borovlev, Y.A.; et al. The CUPID-Mo experiment for neutrinoless double-beta decay: performance and prospects. *Eur. Phys. J. C* **2020**, *80*, 1–15.
 24. Pandey, I.R.; Karki, S.; Kim, H.J.; Kim, Y.D.; Lee, M.H.; Ivannikova, N. V. Luminescence and Scintillation properties of novel disodium dimolybdate ($\text{Na}_2\text{Mo}_2\text{O}_7$) single crystal. *IEEE Trans. Nucl. Sci.* **2018**, *65*, 2125–2131.
 25. Pattavina, L.; Beeman, J.W.; Clemenza, M.; Cremonesi, O.; Fiorini, E.; Pagnanini, L.; Pirro, S.; Rusconi, C.; Schäffner, K. Radiopurity of an archaeological Roman lead cryogenic detector. *Eur. Phys. J. A* **2019**, *55*, 0–5.
 26. Karki, S.; Aryal, A.; Gileva, O.; Kim, H.J.; Kim, Y.; Lee, D.Y.; Park, H.K.; Shin, K. Reduction of radioactive elements in molybdenum trioxide powder by sublimation method and its technical performance. *J. Instrum.* **2019**, *14*, T11002.
 27. Lutterotti, L.; Matthies, S.; Wenk, H.R.; Schultz, A.S.; Richardson, J.W. Combined texture and structure analysis of deformed limestone from time-of-flight neutron diffraction spectra. *J. Appl. Phys.* **1997**, *81*, 594–600.
 28. Brun, R.; Rademakers, F. ROOT - An object oriented data analysis framework. *Nucl. Instruments Methods Phys. Res. Sect. A Accel. Spectrometers, Detect. Assoc. Equip.* **1997**, *389*, 81–86.
 29. Groenink, J.A.; Blasse, G. Some new observations on the luminescence of PbMoO_4 and PbWO_4 . *J. Solid State Chem.* **1980**, *32*, 9–20.
 30. Kajitani, T.; Itoh, M. Time-resolved composite nature of the self-trapped exciton luminescence in

- PbMoO₄. *Phys. Status Solidi Curr. Top. Solid State Phys.* **2011**, *8*, 108–111.
31. Mihokova, E.; Nikl, M.; Bohacek, P.; Babin, V.; Krasnikov, A.; Stolovich, A.; Zazubovich, S.; Vedda, A.; Martini, M.; Grabowski, T. Decay kinetics of the green emission in PbWO₄:Mo. *J. Lumin.* **2003**, *102–103*, 618–622.
 32. Spassky, D.A.; Nagirnyi, V.; Mikhailin, V. V.; Savon, A.E.; Belsky, A.N.; Laguta, V. V.; Buryi, M.; Galashov, E.N.; Shlegel, V.N.; Voronina, I.S.; et al. Trap centers in molybdates. *Opt. Mater. (Amst)*. **2013**, *35*, 2465–2472.
 33. Buryi, M.; Laguta, V.; Fasoli, M.; Moretti, F.; Jurek, K.; Trubitsyn, M.; Volnianskii, M.; Nagorny, S.; Shlegel, V.; Vedda, A.; et al. Charge trapping processes and energy transfer studied in lead molybdate by EPR and TSL. *J. Lumin.* **2019**, *205*, 457–466.
 34. Buryi, M.; Laguta, V.; Fasoli, M.; Moretti, F.; Trubitsyn, M.; Volnianskii, M.; Vedda, A.; Nikl, M. Electron self-trapped at molybdenum complex in lead molybdate: An EPR and TSL comparative study. *J. Lumin.* **2017**, *192*, 767–774.